ISSN: 2319-5967
ISO 9001:2008 Certified
International Journal of Engineering Science and Innovative Technology (IJESIT)
Volume 2, Issue 1, January 2013

On a Two Pole Motor for Electric Propulsion System

M. Leijon, B. Ekergård, S. Apelfrojd, J.de Santiago, H. Bernhoff, R. Waters and S. Eriksson Swedish Centre for Renewable Electric Energy Conversion, Div of Electricity, Dept of Engineering Science, Uppsala University, Sweden

Abstract*— Recent development of "All Electric Vehicle" and "All Electric Propulsion System" has been devoted to four, six and eight pole electric machines. This has primarily been due to existing technology and existing trends. In the present paper we present results from a high speed permanent magnet two pole machine with variable frequency, which can have an impact of the whole electric propulsion system .The simulation results indicate an improvement on the working efficiency and facilitate on the mechanical design. The design can thereby offer a more sustainable and cost-effective electric motors in the range of 20 kW to 1 MW used in electric propulsion systems. The first prototype is constructed and initial experiments with the rotating motor and its control system has been performed.

***Index Terms*— Propulsion System, All Electric Drive, Permanent Magnet Motors.**

I. INTRODUCTION

During several years car manufacturers have developed hybrid and electric solutions for propulsion systems [1]-[3]. In an overall survey, most frequently four, six or eight pole electric motors, with rather poor efficiency, below 95%, are used [4]- [9], However, with the solution of Maxwell's equations or "full physics" as opposed to equivalent circuits (Park), as is normally taught and used world wide, it is realized that for high speed drives the smaller amount of poles the more compact and cost efficient the generator or motor can be. The variable speed motor, designed with Nd-Fe-B-magnets, the paper presents is designed to achieve a high electrical efficiency in a frequency interval from 0 – 50 Hz, with the intention to thereby reduce the requirement of a gearbox. The total efficiency and mechanical stability of the system can thereby be increased. The numerical calculations done with rotational finite element methods (FEM) are described in the theory section. This type of complex full physics calculation have been verified in many real existing motors and generators – like Porjus 45kV 10 MW, Porsi 155 kV 55MW, Eskilstuna 132 kV 32 MW, Troll 40 kV 40 MW and more. [10]- [12]

II. THEORY

A. *Electromagnetic Model*

Electromagnetic simulations using FEM are performed in order to simulate the motor's behaviour at different loading conditions. In the simulations the electromagnetic field inside the motor is assumed to be axi-symmetrical and is therefore modelled in two dimensions. Three-dimensional effects such as end region fields are taken into account by introducing coil end impedances in the circuit equations of the windings. The permanent magnet is modelled by a surface current source.

The electromagnetic model is described by a combined field and circuit equation model. The field equation, (1), originates from Maxwell's equations

$$\sigma\frac{\partial A_z}{\partial t}-\nabla\cdot\left(\frac{1}{\mu_0\mu_r}\nabla A_z\right)=-\sigma\frac{\partial V}{\partial z} \tag{1}$$

and σ is the conductivity, μ_0 and μ_r are vacuum and relative permeability respectively, A_z is the axial magnetic potential and $\partial V/\partial z$ is the applied potential. The circuit equations are described by

$$I_a+I_b+I_c=0$$

$$U_{ab}=U_a+R_sI_a+L_s^{end}\frac{\partial I_a}{\partial t}-U_b-R_sI_b-L_s^{end}\frac{\partial I_b}{\partial t} \tag{2}$$

$$U_{cb}=U_c+R_sI_c+L_s^{end}\frac{\partial I_c}{\partial t}-U_b-R_sI_b-L_s^{end}\frac{\partial I_b}{\partial t}$$

ISSN: 2319-5967
ISO 9001:2008 Certified
International Journal of Engineering Science and Innovative Technology (IJESIT)
Volume 2, Issue 1, January 2013

where I_a, I_b, I_c are the conductor currents, U_{ab} and U_{cb} are the terminal line voltages, U_a, U_b, U_c are the terminal phase voltages obtained from solving the field equation, R_s is the cable resistance and L_s^{end} represents the coil end inductance. After the geometry is set, the motor parts are assigned different material properties such as conductivity, permeability, density, sheet thickness etc. The electromagnetic model is solved in the finite element environment ACE [13]. The mesh is finer close to critical parts such as the airgap and coarser in areas like the yoke of the stator. Simulations can be performed either in a stationary mode where the results are given for a fixed rotor position or in a dynamic mode including the time-dependence and thereby giving more accurate results. The simulation method has been verified by comparison with experimental results for different generators [14]- [17],

B. Electromagnetic Losses and Efficiency

The electrical efficiency, η, of a motor is found from

$$\eta = \frac{P_{el} - P_{losses}}{P_{el}} \quad (3)$$

Where P_{el} is the electrical input power and P_{losses} are the total electromagnetic losses found from.

$$P_{losses} = P_{Fe} + P_{Cu} + P_{Rotor} \quad (4)$$

Where P_{Fe} are the iron losses, P_{Cu} are the copper losses and P_{Rotor} are the eddy current losses in the rotor iron, see below. The iron losses per cubic meter stator, steel can be found from the following equation [18]- 19]

$$P_{Fe,vol} = k_f k_{hy} B_m^2 f + k_f k_{eddy} (B_m f)^2 + k_f k_{exc} (B_m f)^{1.5} \quad (5)$$

Where k_f is the stacking factor, k_{hy} is the hysteresis losses coefficient, k_{eddy} is the eddy current losses coefficient, k_{exc} is the excess losses coefficient, B_m is the peak magnetic flux density and f is the frequency. Rotational losses are omitted. The eddy current losses coefficient can be calculated according to

$$k_{eddy} = \pi^2 \frac{\sigma d^2}{6} \quad (6)$$

Where σ is the conductivity and d is the steel thickness, so the eddy current losses are dependent on the steel thickness squared and can be decreased by choosing thinner steel plates. The coefficients for hysteresis and excess losses, k_{hy} and k_{exc} are found from the loss characteristics specified from the steel manufacturer [20]. The iron losses have to be multiplied with the total stator steel volume, V, and a loss correction factor to find the total losses.

$$P_{Fe} = 1.5 \cdot P_{Fe,vol} V \quad (7)$$

In the simulations an empirical loss correction factor of 1.5 is used for all iron losses. The loss correction factor represents differences in the theoretical modelling of iron losses and experimental measurements, caused for instance by stray losses, and the value of 1.5 is verified for a 12 kW generator in [21].

The copper losses consist of resistive losses and a small amount of eddy current losses in the copper conductors and can be written as

$$P_{Cu} = 3R_s I^2 + P_{Cu}^{Eddy} \quad (8)$$

Where R_s is the cable resistance, I is the current and P_{Cu}^{Eddy} denotes the eddy current losses in the conductors. The eddy current losses in the cables, induced by the magnetic field inside the conductor, originate from current in the conductor itself, current in nearby conductors and the motors' main magnetic circuit [22], are included in the simulations. The variation of the permeance in the air gap rises from stator slotting and the armature reaction results in a non sinusoidal flux density wave form in the air gap. The flux harmonics rotates with a phase shift referring to the rotor and its derivative induces eddy currents in all conductive parts of the rotor with a skin depth, δ , equal to (9): [23]

$$\delta = \sqrt{\frac{2}{\omega \sigma \mu_0 \mu_r}} \quad (9)$$

ISSN: 2319-5967
ISO 9001:2008 Certified
International Journal of Engineering Science and Innovative Technology (IJESIT)
Volume 2, Issue 1, January 2013

σ is the conductivity of the steel, μ_0 is the permeability in vacuum and μ_r represents the relative permeability of the steel. A rotor with solid poles is from a construction point of view a more suitable choice, increasing the mechanical stability and reducing the production cost. In such a design, the solid pole thickness is much greater than the skin depth, δ. The induced eddy current distribution is here not limited to lack of space and high resistivity as in a laminated design, but mainly by the effect of its own field. The currents are said to be inductance-limited and can thereby *not* be calculated by (5) and (6). The authors have chosen to work with Gibbs' theory to analytical calculated the eddy current loss in the solid poles. The ttheorem states that the non sinusoidal flux density wave can be approximated to a one dimensional field and the reaction effect from the induced eddy currents on the main field can be ignored [24]- [25]. For more information about Gibbs' theory, see [24]- [25], where the analytical calculations have been verified with both experimental and numerical calculations at different level of saturation. No magnet losses are included in the calculations since the magnets are embedded and due to Lenz's Law, no significant magnet losses are expected. Windage losses are included in the simulations and constitute about 0.07% of the total losses at 50 Hz but are not included in the calculation of the electrical efficiency.The mechanical losses in a direct driven electric machine, consisting of friction in couplings and bearings, are usually small. Here, mechanical losses are not considered.

III. MOTOR DESIGN, SIMULATIONS AND ANALYTICAL CALCULATIONS

Literature presents a wide distribution on the power rating of motors designed for electric propulsion systems [26]. The authors argues for a relatively small power rating on the first prototype, due to close related ongoing research, [27], where one acceptable drive-cycle is investigated and presented a nominal power consumption around 4 kW whereas the maximum value reached 34 kW. The rotational speed at the rated power is chosen with the motor directly connected, alternative with a differential with a gear ratio 2:1, to small vehicular wheels in mind. The chose to work with cable winding is done with the physical background of Maxwell, Poynting and Slepian in mind. [12] Presents detailed studies of the electromagnetic stresses on different shapes of conductors, all with strongly benefits of the circular conductor.The authors' main priorities have been the machine's weight, efficiency and ability to offer a stable operation both at rated load and overload with both magnetic and thermal overcapacities. By limiting the RMS, line-to-line voltage level to maximum 350 V, the DC-voltage can be restricted to below 1 kV, and thereby enable use of standard components in the chosen two-level IGBT-inverter, controlled by Pulse Width Modulation.

The electromagnetic simulations of the AC motor are performed by using the model described in section 2.1. Dynamic simulations are used. The efficiency is modelled according to the theory described in section 2.2. The motor has been simulated with a varying rotational speed and a varying load sweeping through a wide range of values to cover the whole operational interval as well as extreme cases of overload at higher loading than expected during normal operation. The eddy current losses in the rotor are calculated with the analytical equations presented in the same section and are included in the presented results.

IV. RESULTS

A. *Mechanical and Electrical Design*

The main dimension of the motor design is presented in Table I, whereas the main electrical parameters are presented in Table II.

TABLE I .MAIN DESIGN PARAMETERS OF THE MOTOR

No of Stator Phases	3
Slots/Pole and Phase	7
Coil Pitch	18
Outer Stator Radius [mm]	165
Outer Rotor Radius [mm]	75
Length [mm]	180
Weight stator iron [kg]	68.1
Weight rotor iron [kg]	12.6
Weight magnet [kg]	9.6
Stator steel	M250-35A
Specific loss density for M250-35A	2.35 W/kg at 1.5 T

ISSN: 2319-5967
ISO 9001:2008 Certified
International Journal of Engineering Science and Innovative Technology (IJESIT)
Volume 2, Issue 1, January 2013

TABLE II. DESIGN CASES FOR THE SIMULATED MOTOR

	No Load	Full Load	100 % Overload due to the current
Power [kW]	0	30	60
Current density [A/mm^2]	0	3.3	6.6
Frequency [Hz]	50	50	50
Power Factor	-	1	1
Load angle [°]	0	20.8	35

B. Simulated and Calculated Data

The geometry can be seen in Fig 1 and Fig 3. The permanent magnet is in the design located in the middle of the rotor. The motor's flux density at three different loads is presented in Fig 1.

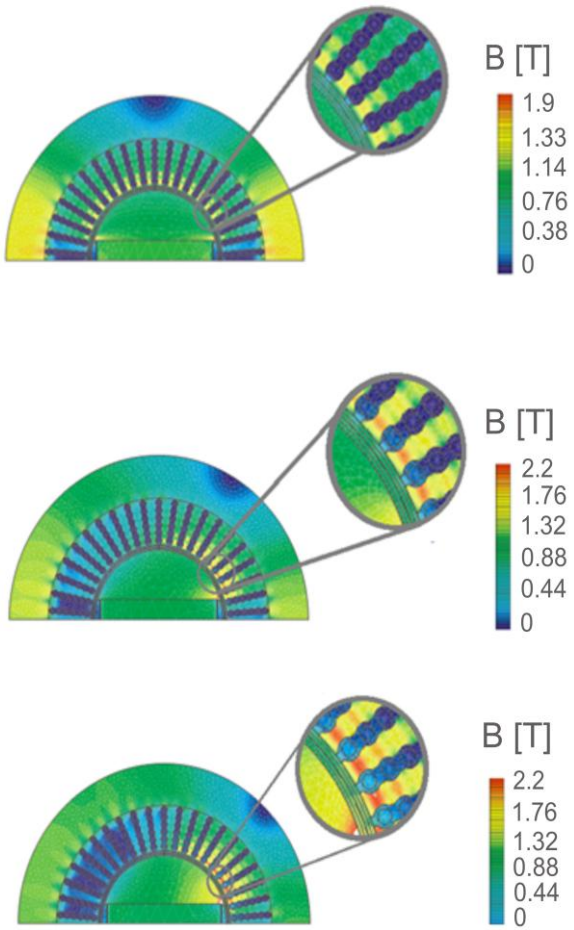

Fig. 1: The magnetic flux density at:
a) No Load b) Full Load c) 100 % Overload.

The variation of the magnetic flux density in the air gap at three different loads is presented in Fig 2.

ISSN: 2319-5967
ISO 9001:2008 Certified
International Journal of Engineering Science and Innovative Technology (IJESIT)
Volume 2, Issue 1, January 2013

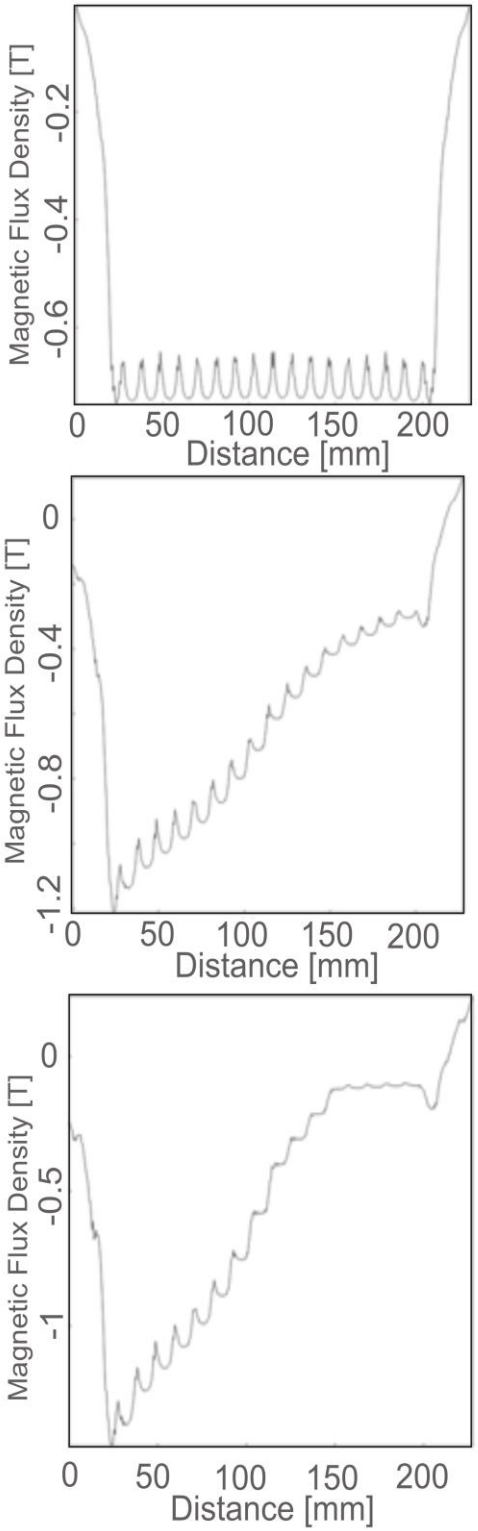

Fig. 2: The magnetic flux density variation in the air-gap at: a) No Load b) Full Load c) 100 % Overload.

The rotor's mechanical resonance frequencies' is presented in Table III, whereas Fig 3 present the graphical view of the stresses in the rotor structure at 3000 RPM.

ISSN: 2319-5967
ISO 9001:2008 Certified
International Journal of Engineering Science and Innovative Technology (IJESIT)
Volume 2, Issue 1, January 2013

TABLE III .THE RESONANCE FREQUENCY

No	Numerical Calculations [Hz]	Analytical Calculations [Hz]
0	0	0
1	1667	2156
2	-	8626

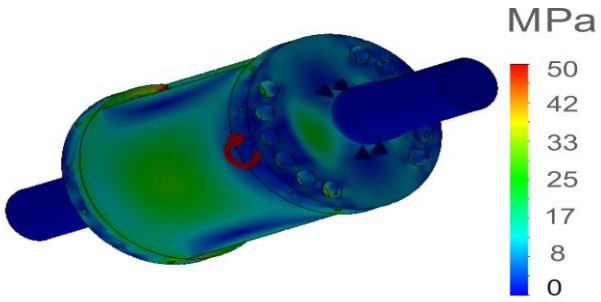

Fig. 3. The stresses on the structure at 3000 RPM.

Calculations for the eddy current losses in a solid-pole rotor at 50 Hz are presented in Table IV. Material data for steel EN 24 was used in the calculations. For definitions of the parameters, see [24], Fig 2-4.

TABLE IV .THE RESULTS FROM THE ANALYTICAL CALCULATIONS

	No Load	Full Load	100 % Overload
Flux oscillation factor	0.05	0.05	0.05
Harmonic factor	1.1	1.1	1.1
$H_{tangential}$ [A/m]	591	940	1293
P_{Rotor}^{Eddy} [W]	22.5	42.1	58

The numerical and analytical calculations of the operating characteristic of the machine are presented in Fig 4-5. Fig 4 presents the results for the permanent magnet motor from nominal to rated load with the control-strategy Scalar Control.

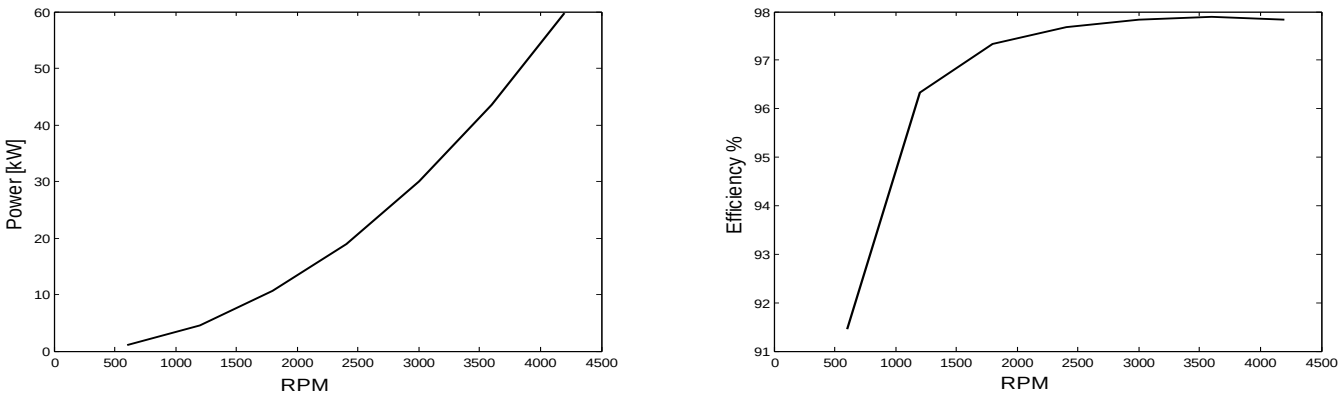

Fig. 4. From left to right, a) The motor's power and b) the electromagnetic efficiency.

ISSN: 2319-5967
ISO 9001:2008 Certified
International Journal of Engineering Science and Innovative Technology (IJESIT)
Volume 2, Issue 1, January 2013

As stated in Section III, one goal is to implement the motor directly connected, alternative with a differential with a gear ratio 2:1, to the wheels of a small vehicular. As the voltage is set by the electrical frequency, the delivered power can be controlled by the amplitude of the current in the circuit, i.e. the machine can be under- and overloaded. Therefore, to investigate the design in a more realistic case, Fig 5 present the motor's performance with help of efficiency maps at different load conditions.

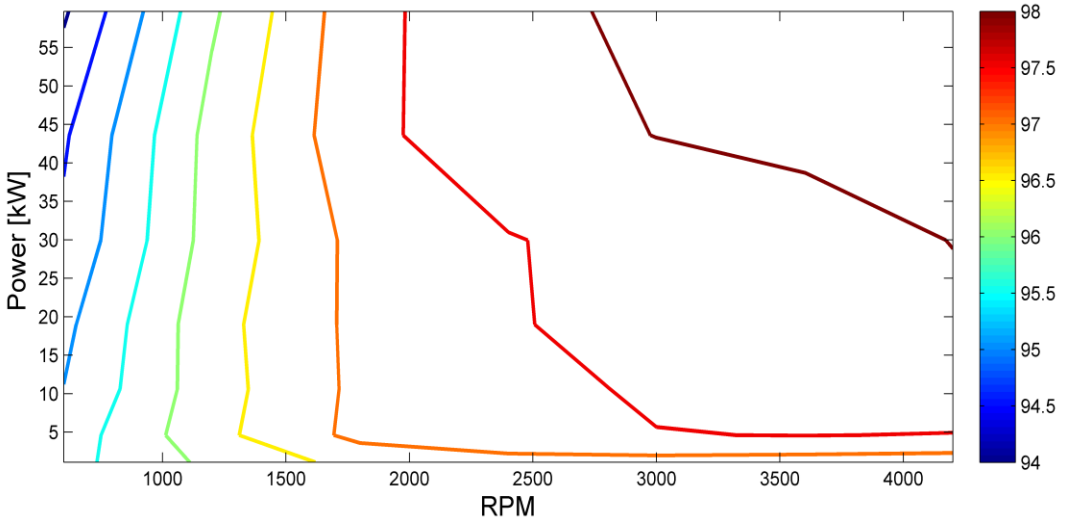

Fig. 5. Efficiency map for different load conditions

C. Experimental Prototype

As a first step of the experimental work, the first prototype has been designed, constructed and assembled. Fig 6 presents the two-pole rotor.

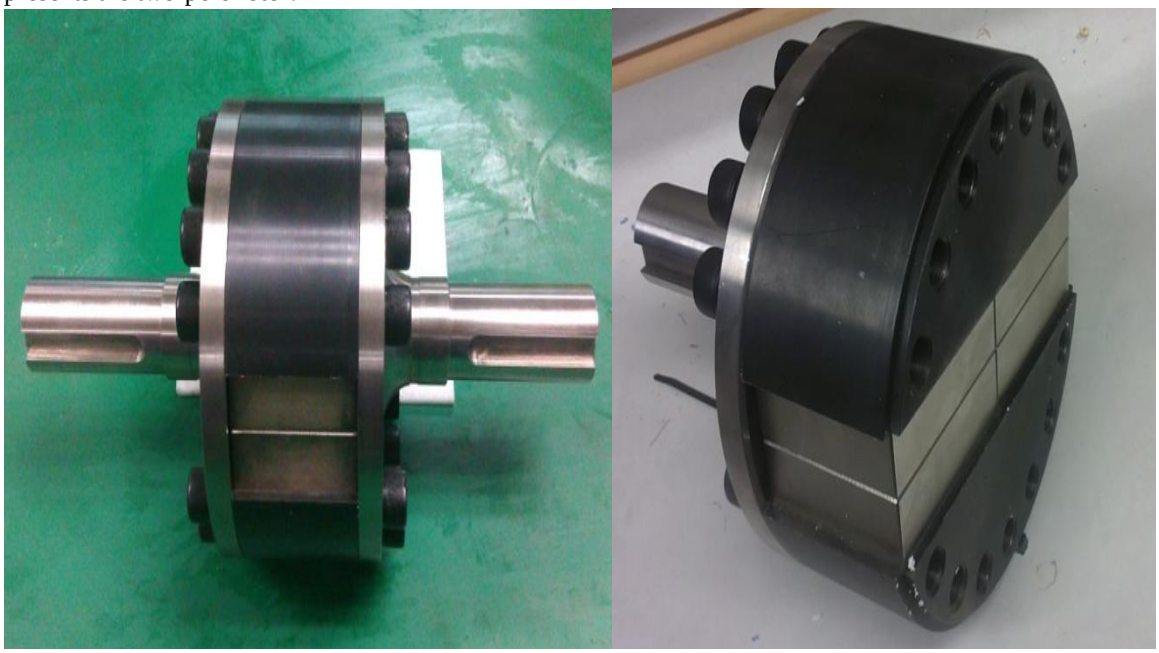

Fig. 6. The Two-Pole Rotor, Where the Gray Magnets are Located in The Middle Of the Two Black Pole-Shoes.

The first prototype is further utilized to increase the knowledge of the control system of this saliency pole machine. As stated in Section III, a two-level inverter is integrated in the system, presented in Fig 7.

ISSN: 2319-5967
ISO 9001:2008 Certified
International Journal of Engineering Science and Innovative Technology (IJESIT)
Volume 2, Issue 1, January 2013

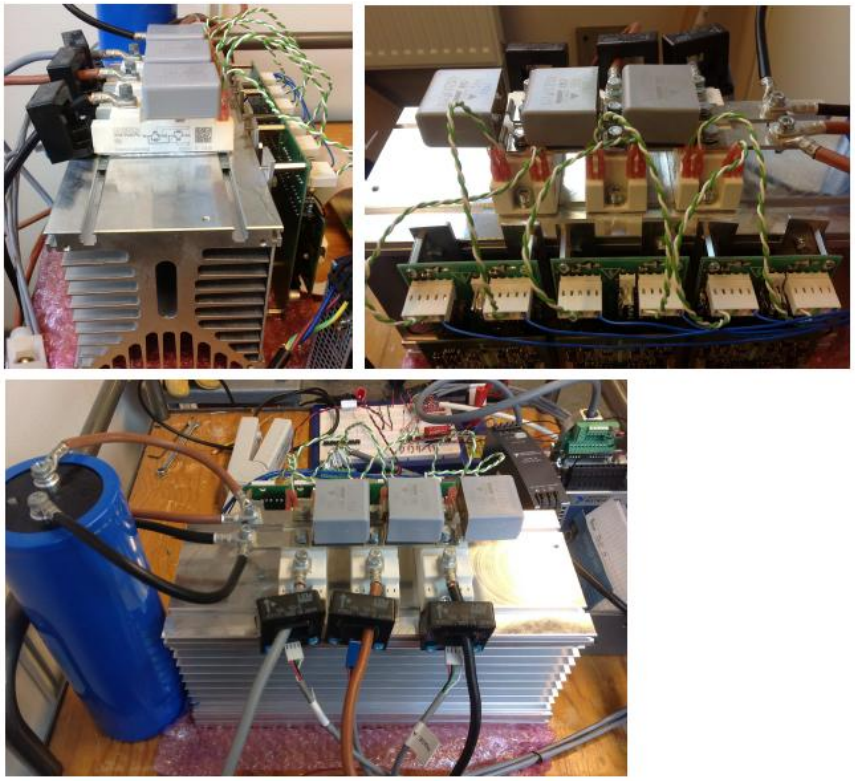

Fig. 7. The Top Pictures Presents The Drive Circuit Connected To The IGBT On The Heat-Sink, Whereas The Lower Picture Shows The Installed Hall-Sensors, Implemented To Measure The Flowing Current.

Initial tests of the control system and inverter have rotated the motor up to 1217 rpm. Fig 8 to Fig. 10 presents the filtered voltage output from the inverter where the motor reach a rotational speed of 367 rpm, 667 rpm resp. 1217 rpm.

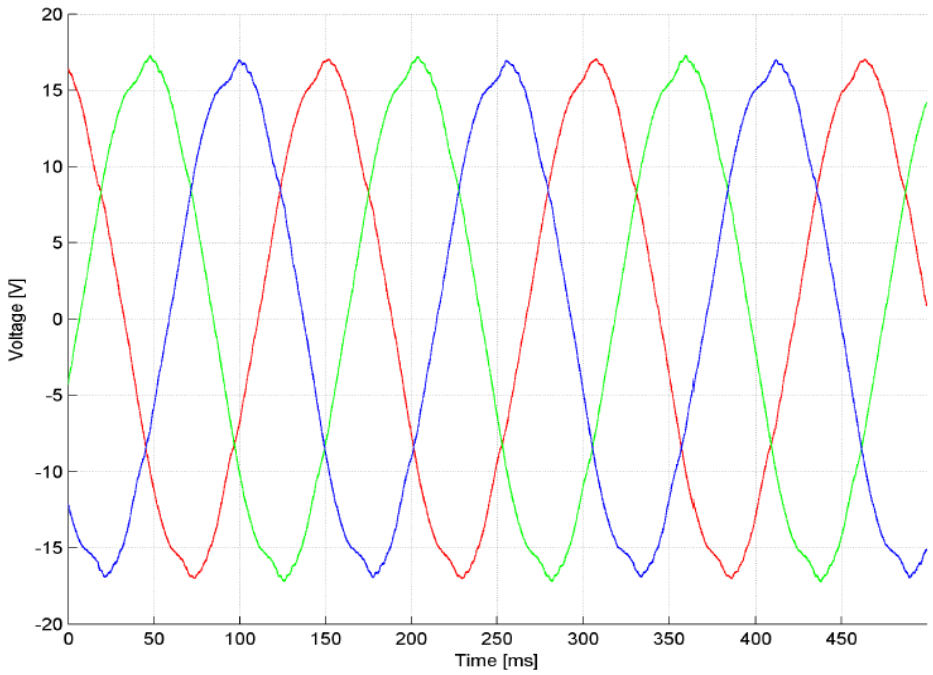

Fig. 8. The line-to-line voltages at 367 rpm.

ISSN: 2319-5967
ISO 9001:2008 Certified
International Journal of Engineering Science and Innovative Technology (IJESIT)
Volume 2, Issue 1, January 2013

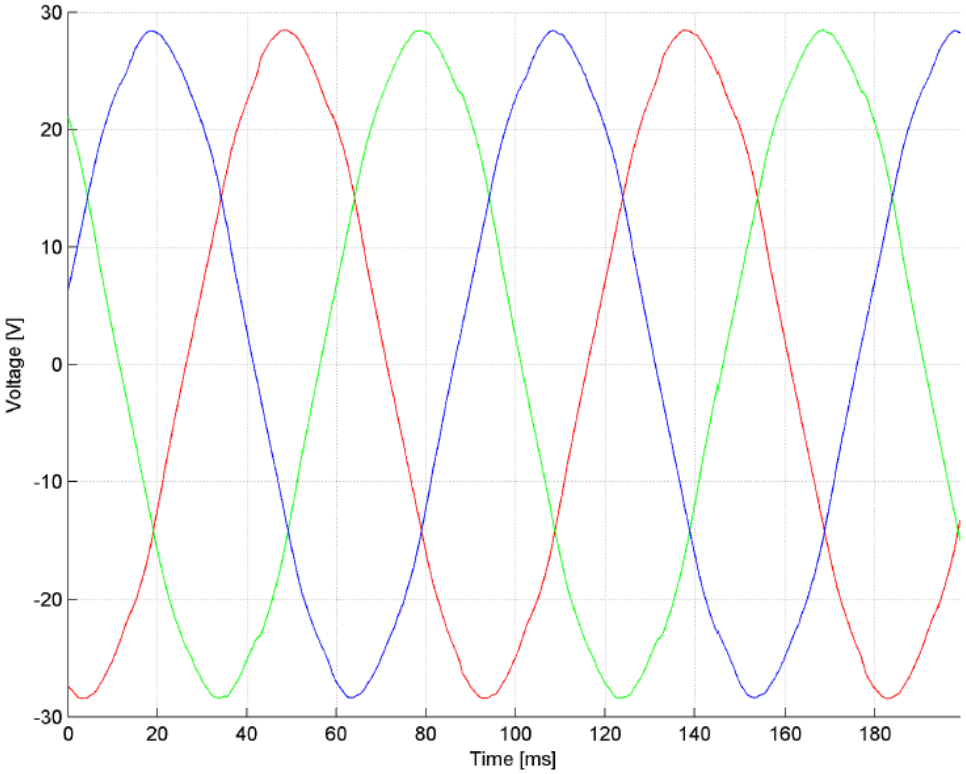

Fig. 9. The line-to-line voltages at 667 rpm.

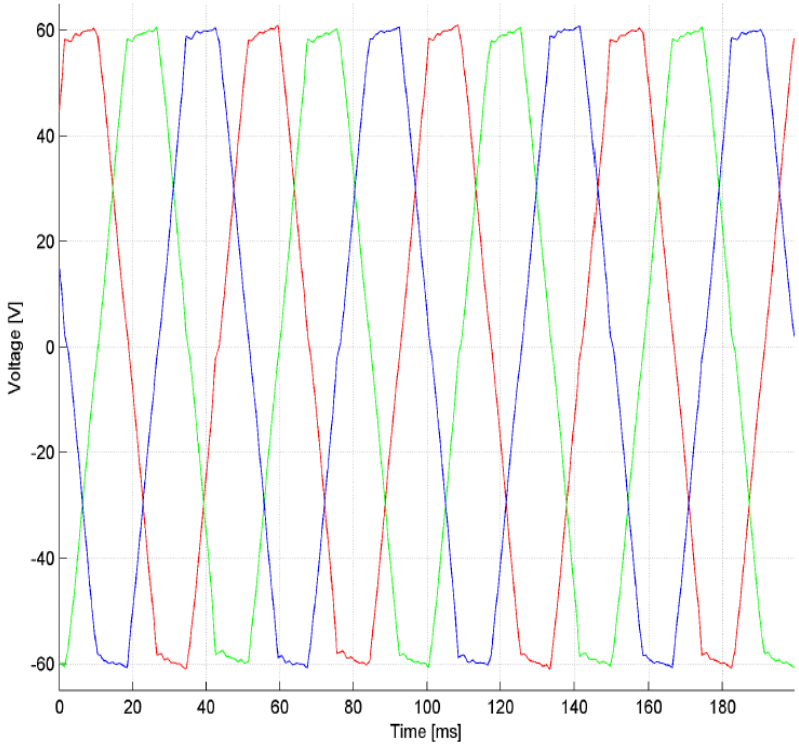

Fig.10. The line-to-line voltages at 1217 rpm.

Fig. 11 presents the ringing of the collector- and the emitter voltage at 5 kHz switching-frequency.

ISSN: 2319-5967
ISO 9001:2008 Certified
International Journal of Engineering Science and Innovative Technology (IJESIT)
Volume 2, Issue 1, January 2013

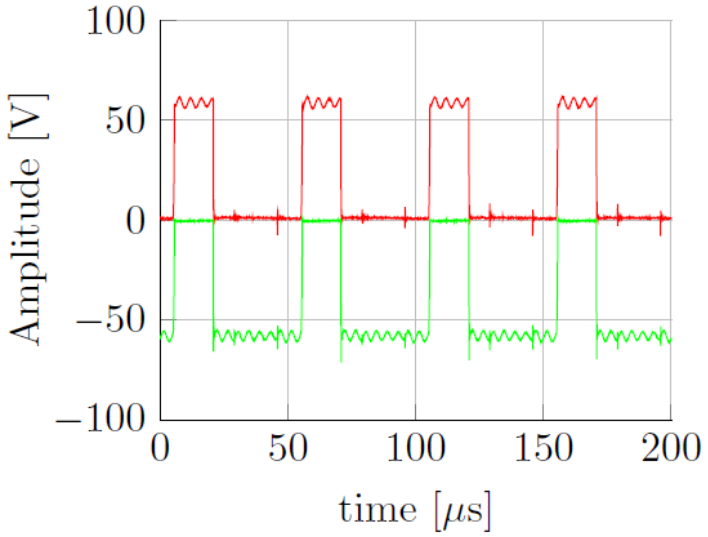

Fig. 11. Measurement of the Ringing With a Switching Frequency of 5 KHz.

V. DISCUSSION

The simulations presents a non sinusoidal flux density wave form in the air gap, see Fig. 2, where the flux harmonics caused by the stator slotting and the armature reaction are clearly visible. Due to the variation of the flux harmonics amplitudes and the non-uniform distribution of the magnetic field, and thereby the permeability in the rotor, accurately analytical calculations of the induced eddy current in the rotor can be difficult to achieve. The maximum value of the magnetic flux density at the rotor, not the mean value as Gibbs' Theory suggests, was used as inputs in the calculations to make sure no under-estimation was taken place. However, based on the experimental verification and the good agreement between the analytical and numerical calculated results at low saturation presented in [24] – [25], the authors believes the theorem gives a good estimation of the size of the rotor-losses in the presented motor. The authors have thereby chosen to construct a rotor with solid poles for the first prototype for further investigations and experiments, see Fig. 6.

The eddy current losses in the conductors constitute a quite large part of the copper losses. However, the simulations are performed with solid, not stranded conductor. The eddy current induced by external magnetic field is strongly dependent on the resistivity in the conductor's radial direction, and shall hence decrease when stranded conductors are used. As stated above, the core losses due to rotational fields are omitted in the calculations in the same way as the core losses due to leakage flux. Further experimental verification of the analytic and numeric calculations is the next step of the development of the two pole permanent magnet motor.

The authors argue for the importance of testing the motor during realistic conditions with accepted drive-cycles. Fig. 5 presents an efficiency map over the operating area, but it does not specify the operation sequence of an electric vehicular.

By increasing or decreasing the loading, the current and thereby the torque can be increased or decreased without accelerate the machine. The cable manufacturer guarantees stable cable insulation up to 6 A/mm^2 at passive air-cooling. Due to high working electrical and electromagnetic efficiency the authors argues for remove the normally utilized axial water-cooling system and thereby further increase the mechanical stability. However, the heating system in the car has thereby to be solved in another way.

The electromagnetic design of the motor results in a relatively low load angle, presented in Table II and Fig. 1-2. With this information, the authors have chosen not to focus on the field weakening at this early stage of the project. However, studies are planned and the authors argue for adjustment in the inverter's control code for a correct utilization of the salient pole motor.

The mechanical construction is designed for allowing a maximum stress at 70 MPa. According to the material parameters for the selected materials, stresses in those sizes shall not result in any risk of fatigue of the rotating part of the motor.

ISSN: 2319-5967
ISO 9001:2008 Certified
International Journal of Engineering Science and Innovative Technology (IJESIT)
Volume 2, Issue 1, January 2013

The chosen inverter is a two level IGBT-inverter, controlled by Pulse Width Modulation. The output signal's harmonics converge around multiples of the switching frequencies. A passive filter, located between the inverter and motor shall reduce these harmonics. Despite this, the inverter's switching frequency has to be chosen with the rotor's resonance frequency in mind. [28]

The switching measurement, see Fig. 11, presents a low voltage ringing. However, if the ringing exceeds the rated voltage of the IGBT at higher voltage and currents, the phenomena could cause problem. Possible solutions if the problem increases can be to reduce stray inductance in the power supply circuit, integrate further protection-components or reduce the switching-time. However, more losses would be introduced in the system, and the best solution it therefore left for further investigation.

The authors plan to further investigate the value of the design frequency, in this case 50 Hz. By studying Faraday's Law of Induction, it is clearly seen that the motor's size is reduced if a higher design frequency is chosen. However, if the motor is directly connected to the car's wheel, i. e. no gearbox is used, a to high design frequency results in a larger operation frequency interval for the motor. The time the motor is driven in non-optimal operation increases, with all the following drawbacks. Different design frequency for different ratings, purpose and requirements is of course a possibility.

VI. Conclusion

We have presented an electric motor with high efficiency over a wide frequency operation interval. Comparison between the simulated motor and existing, full scale motors used in electrical vehicles show a substantial possibility to increase the electrical and overall efficiency in an All Electric Propulsion System. A higher efficiency is saving not only energy but also cooling equipment and a simpler and more stable overall system-design is reached. Our design approach is to simulate the machine's conditions stepwise by numerical calculation methods, directly based on Maxwell's equations. This type of complex full physics calculation have been verified in many real existing motors and generators – like Porjus 45kV 10 MW, Porsi 155 kV 55MW, Eskilstuna 132 kV 32 MW and Troll 40 kV 40 MW etc. The first prototype is assembled and has been rotated up to 1217 rpm

Acknowledgment

The authors would like to express gratitude's to Dr Arne Wolf Brandt and Dr Urban Lundin for their support with the simulation tool and Anders Kronberg is acknowledged for help with the inverter setup.

REFERENCES

[1] Koch AK, Fowler MW, Fraser RA. Implementation of a fuel cell plug-in hybrid electric vehicle and factors affecting transportation policy. International Journal of Energy Research, 23 SEP 2011, DOI: 10.1002/er.1907.

[2] Chan CC. The State of the Art of Electric and Hybrid Vehicles. Proceedings of the IEEE, Vol. 90, No. 2, pp. 704-718, Feb. 2002

[3] Zeraoulia M, Benbouzid MEH, Diallo D. Electric Motor Drive Selection Issues for HEV Propulsion Systems: A Comparative Study. IEEE Transactions on vehicular Technology, Vol. 55, No. 6, pp. 8, November 2006.

[4] Finken T, Hombitzer M, Hameyer K. Study and Comparison of several Permanent-Magnets excited Rotor Types regarding their Applicability in Electric Vehicles. Emobility – Proc. VDE-Kongress 2010, November 2010.

[5] Choi JH, Chun YD, Han PW, Kim MJ, Koo DH, Lee J, Chun JS. Design of High Power Permanent Magnet Motor with Segment Rectangular Copper Wire and Closed Slot Opening on Electric Vehicles. IEEE Transactions on Magnetics, Vol. 46, No. 9, pp. 3701 – 3704, September 2010.

[6] Zhang Z, Profumo F, Tenconi A. Improved design for electric vehicle induction motors using an optimization procedure. IEE Proc.-Electr. Power Appl., Vol. 143, No. 6, pp. 21 – 25, November 1996.

[7] Shuanghong W, Qionghua Z, Zhiyuan M, and Libing Z. Implementation of a 50-kW Four-Phase Switched Reluctance Motor Drive System for Hybrid Electric Vehicle. IEEE Transactions on Magnetics, Vol. 41, No. 1, pp. 501 – 504, January 2005.

[8] Lukic SM, Emado A. Modeling of electric machines for automotive applications using efficiency maps. Proc. Electrical Insulation Conference and Electrical Manufacturing & Coil Winding Technology Conference, pp. 543 – 550, 2003.

ISSN: 2319-5967
ISO 9001:2008 Certified
International Journal of Engineering Science and Innovative Technology (IJESIT)
Volume 2, Issue 1, January 2013

[9] Rahman KM, Fahimi B, Suresh G, Rajarathnam AV, Ehsani M. Advantages of Switched Reluctance Motor Applications to EV and HEV: Design and Control Issues. IEEE Transactions on Industry Applications, Vol. 36, No. 1, pp. 111 - 121, Jan/Feb 2000.

[10] Leijon M.Powerformer – a radically new rotating machine. ABB Review 2/1998 pp. 21-26.

[11] Leijon M, Dahlgren M, Walfridsson L, Ming L, Jaksts A. A recent development in the electrical insulation systems of generators and transformers. IEEE Electrical Insulation Magazine, Vol. 17 No. 3, pp. 10 -15, May-June 2001.

[12] Bolund B, Leijon M and Lundin U. Poynting Theorem applied to Cable Wound Generators. IEEE Transaction on Dielectrics and Electrical Insulation, Vol. 15, No. 2, pp. 600-605, April 2008.

[13] Anon. 1. Ace, Modified Version 3.1, ABB common platform for field analysis and simulations. ABB Corporate Research Centre. ABB AB, Corporate Research, 721 78 Västerås, Sweden.

[14] Eriksson S, Solum S, Bernhoff H, Leijon M. Simulations and experiments on a 12 kW direct driven PM synchronous generator for wind power. Renewable Energy, Vol. 33 No.4, pp. 674-681, 2008.

[15] Eriksson S, Bernhoff H, Leijon M. FEM simulations and experiments of different loading conditions for a 12 kW direct driven PM synchronous generator for wind power, International Journal of Emerging Electric Power Systems, Vol. 10, No. 1, article 3, 2010.

[16] Eriksson S, Bernhoff H, Leijon M. A 225 kW direct driven PM generator adapted to a vertical axis wind turbine. Advances in Power Electronics, Volume 2011 (2011), Article ID 239061, doi:10.1155/2011/239061.

[17] Leijon M, Bernhoff H, Ågren O, Isberg J, Sundberg J, Berg M, Karlsson KE., Wolf Brandt A. Multiphysics Simulation of Wave Energy to Electric Energy Conversion by Permanent Magnet Linear Generator. IEEE Transactions on Energy Conversion, Vol. 20, No 1, pp. 219 – 224, March 2005.

[18] Broddefalk A, Lindenmo M. Dependence of the power losses of a non-oriented 3% Si-steel on frequency and gauge. Journal of Magnetism and Magnetic Materials, Vol. 304, No. 2, pp. 586-588, September 2006.

[19] Mi CC, Slemon GR, Bonert R. Minimization of iron losses of permanent magnet synchronous machines. IEEE Transactions on Energy Conversion, Vol. 30, No. 1, pp. 121-127, March 2005

[20] Anon. 2. Electric Steel Non Oriented Fully Processed Cogent, Cogent 2002-11. SIR-Gruppen Sweden, Surahammars Bruk AB, Box 201, SE-735 23 Surahammar, Sweden.

[21] Bülow F. Extreme Load Conditions for Wind Powered Direct Drive PM Generators. Licentiate thesis, Uppsala University, UURIE 324-11L, Uppsala 2011,.

[22] Holmberg P, Leijon M, Wass T. A Wideband Lumped Circuit Model of Eddy Current Losses in a Coil with a Coaxial Insulation System and a Stranded Conductor. IEEE Transactions on Power Delivery, Vol. 18, No. 1, pp. 50-60, January 2003.

[23] Stoll RL, The analysis of eddy currents. Oxford University Press, 1974.

[24] Drubel O, Stoll RL. Comparison between Analytical and Numerical Methods of Calculating Tooth Ripple Losses in Salient Pole Synchronous Machines. IEEE Transactions on energy conversion, Vol. 16, No. 1, pp. 61-67, March 2001.

[25] Gibbs WJ. Tooth-ripple losses in unwound pole-shoes. Journal of the Institution of Electrical Engineers - Part II, Vol. 94, No 37, pp 2. February 1947.

[26] West JGW. DC, induction, reluctance and PM motors for electric vehicles. Power Engineering Journal, vol. 8, no. 2, pp. 77-88, 1994.'

[27] Santiago J, Goncalves de Oliveira J, Lundin J, Abrahamsson J, Larsson A, Bernhoff H. Design parameters calculation of a novel driveline for electric vehicles. World Electric Vehicle Journal Vol. 3 ISSN 2032-6653 - 2009 AVERE.

[28] Dahlvig G. Konstruktionselement och maskinbyggnad. Liber. 6th Edition, 1999

AUTHOR BIOGRAPHY

Professor Mats Leijon (M'82) received the Ph.D. degree in electrical engineering from Chalmers University of Technology, Gothenburg, Sweden, in 1987. From 1993 to 2000, he was a Head of the Department for High Voltage Electromagnetic Systems, ABB Corporate Research, and Västerås, Sweden. In 2000, he became a Professor of Electricity at Uppsala University, Uppsala, Sweden. He has supervised 18 Dr and 6 Tech Lic and written over 250 papers of which 110 in peer reviewed journals. He has more than 200 original patents ending up into 1417 patents worldwide. Currently, he supervises fourteen Ph.D. students within the Renewable area - Wave power, Marine Current power, and All Electric

ISSN: 2319-5967
ISO 9001:2008 Certified
International Journal of Engineering Science and Innovative Technology (IJESIT)
Volume 2, Issue 1, January 2013

Propulsion System. He is co-editor of Renewable Energy, Journal of Applied Mathematics and IET Renewable Power Generation.
Prof. Leijon received the Chalmers award John Ericsson Medal in 1984, the Porjus International Hydro Power Prize in 1998, the Royal University of Technology Grand Price in 1998, the Finnish Academy of Science Walter Alstrom Prize in 1999, and the 2000 Chalmers Gustav Dahlen Medal. He has also received the Grand Energy Prize in Sweden and the Polhem Prize and the Thureus Prize and 2010 The Björkenska Price at Uppsala University. He is a Member IEEE,IET, WEC and Cigre and elected into the Swedish Royal Academy of Engineering Science (IVA II).

Boel Ekergård received her M.Sc. degree in Energy Systems Engineering in 2009 from Uppsala University, Uppsala, Sweden. She is working towards the Ph.D. degree at the Division for Electricity, Uppsala University, and is involved in a wave energy converter project.

Senad Apelfröjd received the M.Sc. degree in Energy Systems Engineering in 2010 from Uppsala University, Uppsala, Sweden. He is now working towards the Ph.D. degree in engineering physics from Uppsala University, and is involved in a wind energy conversion project.

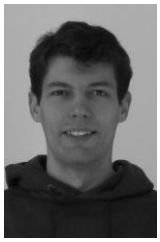

Dr Juan de Santiago was born in Madrid, Spain. Received the M.Sc. in Industrial Engineering from Universidad Polytechnic de Madrid, Spain, in 2005 and the Ph.D in electrical engineering at Uppsala University, Sweden in 2011. He is now researcher specialized in electric machines for energy storage applications.

In 2005 he join the engineering company Empresarios Agrupados, working with solar energy for hydrogen and electricity production. In 2006 he was with the Spanish transmission and electricity system operator Red Electrica the España until he joined Uppsala University.

Professor Hans Bernhoff was born in Umeå, Sweden, in 1964. He has an MSc in Engineering Physics (1988) and a PhD degree in material physics, high temperature superconductors , from the Royal Institute of Technology, Stockholm, Sweden, in 1992. He then held a Postdoctoral position with the IBM Research Laboratory, Rueschlikon, Switzerland.

In 1993, he joined ABB Corporate Research, Västerås, Sweden, where he was a Project Leader for several innovative projects in the area of electro technology, in particular research on single crystal diamond as a wide band gap semiconductor. In 2001, he became an Associate Professor at Uppsala University, Uppsala, Sweden, where he has focused his research and teaching in the area of renewable energy systems: wave power, wind power and energy storage. He has authored or co-authored more than 40 journal articles, over 20 conference contributions and inventor and co-inventor in over 50 international patents.

Rafael Waters (S'06) received the M.Sc. degree in energy systems engineering and the Ph.D. degree in engineering physics from Uppsala University, Uppsala, Sweden, in 2005 and 2008, respectively.
He is manager of the Department for the design of wave power plants at the wave power company Seabased Industry AB, and is also an assistant senior lecturer at the Division for Electricity at Uppsala University
Dr. Waters received the Bjurzon premium for excellent Ph.D. thesis appointed by the principal of Uppsala University. He also received the Gustafsson price for younger scientists in 2010.

Dr Sandra Eriksson was born 1979 in Eskilstuna, Sweden. She finished her MSc in Engineering Physics at Uppsala University, Sweden in 2003 and studied towards a PhD degree in engineering science with a specialization in science of electricity between 2004 and 2008. She is currently working as assistant professor at Uppsala University. Her main topic of interest is permanent magnet electrical machines.